http://www.jmaterenvironsci.com/

Critical Speed Analysis of Bi-layered Rotating Cylindrical Shells Made of Functionally Graded Materials

I. Fakhari Golpayegani [1*], A.A. Jafari [2]

1. Mechanical Engineering Department, Golpayegan University of Technology, Golpayegan, Iran
2. Mechanical Engineering Department, K.N. Toosi University of Technology, Tehran, Iran

Abstract

This study analyzed the free vibrations and critical speed of rotating bi-layered circular cylindrical shells made of functionally graded materials (FGM). The characteristics of the materials in both layers change continuously according to volume fraction power-law distribution. The Coriolis effects, centrifugal force and initial hoop tension created by the rotation and the Sanders' thin shells theory equations were extracted. The effect of the ratios of length to radius and thickness to radius, the rotation speed of the shell, the composition of the materials in the layers, the power law index and circumferential and longitudinal wave numbers on the backward and forward natural frequencies and critical speed of the shells were investigated. The results indicate that the bi-layered shells improved vibration behavior over single-layered shells of the same thickness. The results were confirmed by comparison with the results of previous studies. The natural frequencies of the results for non-rotating bi-layered FGM cylindrical shells and rotating single-layered FGM shells were compared and confirmed the accuracy of the results.

1. Introduction

Rotating cylindrical shells form critical segments of machines such as jet engines, rockets, missiles, centrifugal filters and offshore drilling systems. The installation of sensitive equipment on these structures which feature high vibrations and resonance can cause them to malfunction. Analysis of free vibrations and critical speed during design can improve the safety and functionality of the shells.

Functionally-graded materials are composed of two or more materials. The characteristics of such materials change in thickness with the type of function to create continuity of the mechanical features. Materials made of a combination of metal and ceramic are the best FGM materials. The high resistance of the ceramic at various temperature gradients, thermal stress, abrasion and oxidation and the toughness and strength of metal can be taken advantage of at the same time.

So far many studies were carried out in regarding the free vibration of the FGM cylindrical shell. Loy et al. [1] analyzed the free vibrations of FGM cylindrical shells made of stainless steel and nickel with simply supported ends conditions. They concluded that the vibrational features of these shells are strongly similar to the shells made of isotropic materials. Pradhan et al. [2] investigated the vibrations of FGM shell with various boundary conditions using Love's thin shells theory and Rayleigh Ritz method. Santos et al. [3] using a kind of semi-analytical finite element model and three-dimensional linear elasticity theory studied the cylindrical shells made of functionally graded materials. Iqbal et al. [4] used wave Propagation method to analyze the vibrational characteristics of the shells made of functionally graded materials with various boundary conditions. Arjangpay et al. [5] studied the free vibrations of the shells made of functionally graded materials with numerical method and using Mesh-less Local Petrov-Galerkin (MLPG) method. They extracted the effects of power law index, geometric parameters and boundary conditions on the natural frequencies. Fakhari and ghorbani., [6] investigated free vibration of FGM thin cylindrical shells under non-uniform linear and nonlinear internal pressure.

Multi-layered FGM cylindrical shells have different uses such as in atomic reactors. Lee et al. [7] studied the vibrations of three-layered shells with isotropic outer layer and the FGM core using Flügge's shell theory. They used two different functions to determine the characteristics of FGM layer. Sofiyev et al. [8] analyzed the vibrations and stability of three layers cone shells with the middle layer made of functionally graded materials. They used Galerkin method to extract the equations and noticed that the important parameters in the vibrations of the shells are the combination of their materials and geometric parameters. Arshad et al. [9] studied the vibrations of the bi-layered cylindrical shells with layers of the different material. One layer is made of FGM material and the second layer is made of isotropic materials. The frequencies of the shells with long and short length and low and high thickness were extracted with changing of non-dimensional geometric parameters. Sepiani et al. [10] analyzed the vibration and the buckling of two-layered shells with the inner layer made of functionally graded materials and the outer layer made of isotropic materials. The shell under their investigation was under the static and periodic combined loading. Arshad et al. [11] studied the vibrations of FGM bi-layered shells made of two separate layers which are assumed to be perfectly bonded in the transverse direction at their interface without slip and their deformation is continuous across the layers interface. Shah et al. [12] analyzed vibrational characteristics of the three layered shells with inner and outer layer of FGM and isotropic middle layer.

One of the important factors regarding the vibrations of the circular cylindrical shell is to determine the point at which the critical speed occurs. At this point the frequency of the shell reaches zero and resonance occurs. At the critical speed any remained imbalance in the shell coordinates with the rotation and causes the increase of the vibrations. Some studies are conducted regarding the critical speed of the shells. Kim and Bert, [13] used a simple theory to analyze the critical speed of the cylindrical shell. Ng and Lam, [14] studied free vibrations and critical speed of circular isotropic shells under constant axial load. Ahmad and Naeem [15] studied the vibration of FGM circular shells using Love's thin shell theory. In that study, to analyze the effect of rotation speed only centrifugal forces were taken into account for facilitation of the equations. Hosseini Hashemi and Khorrami, [16] analyzed free vibrations of cylindrical shells made of functionally graded material by Differential Quadrature Method (DQM). The results extracted by them were compared and confirmed by ABAQUS software. The effect of the power law index and geometric parameters on the natural frequencies were extracted in their study. Daneshjoo et al. [17] studied the analysis of three dimensional vibrations and critical speed of the composite cylindrical shells with orthogonal stiffeners under axial load and pressure. They analyzed the effect of different parameters such as geometric parameters, axial load and pressure on the critical speed of the shells. Hosseini Hashemi et al. [18] presented analytical solution of vibrations and critical speed of the thick circular cylindrical FGM shells using Sander's theory. In their study, were studied the effect of boundary conditions, rotation speed and geometric parameters on the natural frequencies and critical speed. Talebitooti et al. [19] presented the analysis of vibrations and critical speed of FGM shells under the thermomechanic loading using GDQ method. Civalek [20] using the discrete singular convolution (DSC) method, studied the free vibration analysis of rotating truncated conical shells, circular shells and panels. Isotropic, orthotropic, functionally graded materials (FGM) and laminated material cases were considered. Mehrparar [21] analyzed vibration of functionally graded spinning cylindrical shells using higher order shear deformation theory.

Previous studies have not provided accurate analysis of the free vibrations and critical speed of circular cylindrical shells made of multi-layered functionally graded materials, nor have the Coriolis effects, centrifugal and initial hoop tensions been considered. The present study analyzed the critical speed of bi-layered circular cylindrical shells made of functionally graded materials which rotate around their longidunal axes. Both layers are formed of functionally graded materials and the characteristics of the materials change continuously according to the volume fraction power-law distribution. To extract the equations of motion, the Sanders' thin shell theory was used regarding the Coriolis effects, centrifugal forces and initially hoop tension created by rotation. The results were confirmed by comparison with the results of other studies. The natural frequencies were compared with results of previous studies on FGM non-rotating bi-layered cylindrical shells and rotating FGM single-layered shells and show the accuracy of the present study. The effect of the number of layers, environmental modes, longitudinal modes, power law index, composition of shell materials and geometric ratio on the natural frequencies and critical speed of the shells were extracted.

2. FGM material properties

FGM materials are made from a combination of two or more materials. Most of these materials are used in high temperature environments and the properties of these materials are defined as a function of temperature according to the following equation [1]:

$$P = P_0\left(P_{-1}T^{-1} + 1 + P_1 T + P_2 T^2 + P_3 T^3\right) \tag{1}$$

Where P_0, P_{-1}, P_1, P_2 and P_3 are constants at temperature T in Kelvin scale and are fixed for any specific matter. The characteristics of FGM, P related to ingredient properties and volume ratio and defined as follows:

$$P = \sum_{j=1}^{k} P_j V_{fi} \tag{2}$$

$P_j \& V_{fi}$ in the aforementioned equation are the characteristics of materials and volume fraction j. Total volume ratio of materials is equal to one.

$$\sum_{j=1}^{k} V_{fi} = 1 \tag{3}$$

For a cylindrical shell with a uniform thickness h and a reference surface at its middle surface, the volume fraction of the two constituents for a shell having a single FGM layer can be expressed as [11]:

$$V_1 = \left(\frac{2z+h}{2h}\right)^N \qquad V_2 = 1 - \left(\frac{2z+h}{2h}\right)^N \tag{4}$$

Where N is the power law $(0 < N \leq \infty)$. For a bi-layered functionally graded cylindrical shell with the constituent materials M1 and M2 for inner FGM Layer, M2 and M3 for outer FGM layer, the effective material parameters Young's modulus E, Poisson's ratio v and the mass density ρ of both layers are expressed as [11]:

$$E_{fgm}{}^1 = (E_2 - E_1)[(2z+h)/h]^N + E_1 \qquad E_{fgm}{}^2 = (E_3 - E_2)[2z/h]^N + E_2$$

$$\upsilon_{fgm}{}^1 = (\upsilon_2 - \upsilon_1)[(2z+h)/h]^N + \upsilon_1 \qquad \upsilon_{fgm}{}^2 = (\upsilon_3 - \upsilon_2)[2z/h]^N + \upsilon_2 \tag{5}$$

$$\rho_{fgm}{}^1 = (\rho_2 - \rho_1)[(2z+h)/h]^N + \rho_1 \qquad \rho_{fgm}{}^2 = (\rho_3 - \rho_2)[2z/h]^N + \rho_2$$

Where $E_{fgm}{}^1 \upsilon_{fgm}{}^1 \rho_{fgm}{}^1$ and $E_{fgm}{}^2 \upsilon_{fgm}{}^2 \rho_{fgm}{}^2$ correspond to the resultant material properties for inner and outer FGM layers, respectively.
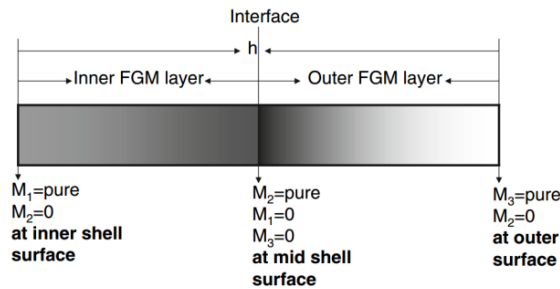
Figure 1: Variation of material properties along the thickness direction of the bi-layered FGM cylindrical shell [9]

Figure 1 shows that material M1 is enriched at the inner surface of the inner layer and is gradually reduced in the thickness direction till it has zero concentration at the outer surface of the inner layer, while material M2 is enriched at the outer surface of the inner layer and has zero concentration at the inner surface of the inner layer. Similarly, in the second layer material M2 is concentrated at the inner surface of the outer layer and has zero concentration at the outer surface of the outer layer, while material M3 is enriched at the outer surface of the outer layer and has zero concentration at the inner surface of the outer layer of the cylindrical shell. The material properties given in Equations (5) are for inner and outer FGM layers of the cylindrical shell which vary from −h/2 to 0 and from 0 to +h/2, respectively. From these relations, it can be concluded that at z =−h/2, the effective material properties become E=E1, v=v1, ρ=ρ1 for inner layer, for z =0, material properties become E=E2, v =v2, ρ=ρ2 in both layers, and at z =+h/2, the material properties turn into E=E3, v = v3, and ρ = ρ3 for functionally graded outer layer of the cylindrical shell. These results lead to the conclusion that there exists a smooth and continuous change in the material properties from material M1 at the inner surface to the material properties of M2 at the outer surface of the shell of the FGM inner layer of the cylindrical shell. Similarly in the outer layer, there is a variation in the material properties from material properties M2 at the inner surface of the outer layer to material properties M3 at the outer surface of the outer layer of the cylindrical shell. Similar behavior is seen in the inverse direction. For this shell, if the thickness to radius ratio is less than 0.05, it will be possible to use the theory of thin shells. In the next section, a formulation based on Sanders' shell theory, for a functionally graded cylindrical shell is carried out.

3. Theory and equations

The main purpose of this section is to obtain the equations of motion for FGM thin cylindrical shell shown in Figure 2, with uniform thickness h, radius R, length L and mass density ρ, which rotates about the x-axis at constant angular velocity Ω. The shell has a coordinate system fixed on its middle surface. Membrane displacement in the longitudinal, circumferential and radial direction (x‹θ‹z) are shown by u, v and w and velocity vectors and displacements of a point on the shell are shown by $\bar{V}$ and $\bar{r}$, respectively. The velocity and displacement vectors at each point of the shell is determined by the following equation.

$$\bar{V} = \dot{\bar{r}}(\Omega = 0) + (\Omega\bar{i} \times \bar{r}) \tag{6}$$

$$\bar{r} = u\bar{i} + v\bar{j} + w\bar{k} \tag{7}$$
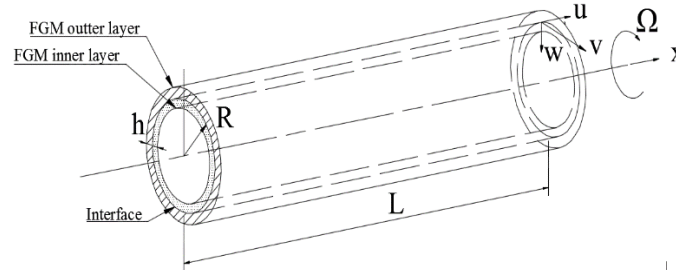
Figure 2: Rotating Bi-layered FGM Cylindrical shell

That $\bar{i}$, $\bar{j}$ and $\bar{k}$ are unit vectors in x and θ and z directions, respectively when $\Omega = 0$. By combining equation (7) with equation (6), the velocity vector is obtained as follows:

$$\bar{V} = \dot{u}\bar{i} + \dot{v}\bar{j} + \dot{w}\bar{k} + (\Omega\bar{i} \times w\bar{k}) + (\Omega\bar{i} \times v\bar{j}) \tag{8}$$

In this equation $\dot{u}$, $\dot{v}$ and $\dot{w}$ are velocity components in three main directions. The kinetic energy of the shell is expressed by following equation [22]:

$$T = \frac{1}{2}h\int_0^L\int_0^{2\pi}\rho_t\,\bar{V}.\bar{V}R\,d\theta\,dx \tag{9}$$

By putting equation (8) into equation (9), the kinetic energy of the shell can be obtained as follows:

$$T = \frac{1}{2}h\int_0^L\int_0^{2\pi}\rho_t\left[\dot{u}^2 + \dot{v}^2 + \dot{w}^2 + 2\Omega(v\dot{w} - w\dot{v}) + \Omega^2(v^2 + w^2)\right]Rd\theta dx \tag{10}$$

Where ρ_t is the mass density per unit length and is defined by:

$$\rho_t = \int_{-H/2}^0 \rho^{fgm1}dz + \int_0^{H/2}\rho^{fgm2}dz \tag{11}$$

Where ρ^{fgm1} and ρ^{fgm2} represent the mass density of the constituent materials in both the FGM layers. The initial hope tension due to the centrifugal force is defined as [22]:

$$N_\theta = \rho h\Omega^2 R^2 \tag{12}$$

The strain energy of the shell due to hoop tension is given as:

$$U_h = \frac{1}{2}\int_0^L\int_0^{2\pi} N_\theta\left\{\left(\frac{1}{R}\frac{\partial u}{\partial\theta}\right)^2 + \left[\frac{1}{R}\left(\frac{\partial v}{\partial\theta} + w\right)\right]^2 + \left[\frac{1}{R}\left(\frac{\partial w}{\partial\theta} - v\right)\right]^2\right\}Rd\theta dx \tag{13}$$

Shell tensile and flexural strain energy can be written as follows [15]:

$$U_\varepsilon = \frac{1}{2}\int_0^L\int_0^{2\pi}\varepsilon^T[S]\varepsilon\,R\,d\theta\,dx \tag{14}$$

In this equation S is the stiffness matrix, and strain vector ε can be written as:

$$\varepsilon^T = \{e_1 e_2\ \gamma\ k_1 k_2\ 2\tau\} \tag{15}$$

In this equation, the middle surface strain is determined by e_1 ‹e_2 and γ and the middle surface curvature is determined by k_1 ‹k_2 and τ.

The formulation in the present study is confined to linear elastic behavior with small displacements and hence small strains. The linear strain- displacement relations according to Sander's shell theory are [23] :

$$e_1 = \partial u / \partial x$$

$$e_2 = -(1/R)(w - \partial v / \partial \theta)$$

$$\gamma = \partial v / \partial x + (1/R)\left(\partial u / \partial \theta\right)$$

$$k_1 = (\partial^2 w)/(\partial x^2)$$

$$k_2 = -(1/R^2)((\partial^2 w)/(\partial \phi^2) - \partial v / \partial \phi)$$

$$\tau = -\left(1/R\right)(\partial^2 w)/\partial x \partial \theta + \left(3/4R\right)\left(\partial v / \partial x\right) - \left(1/4R^2\right)\partial u / \partial \theta \tag{16}$$

Stiffness matrix for shell is given by:

$$[S] = \begin{bmatrix} A_{11} & A_{12} & 0 & B_{11} & B_{12} & 0 \\ A_{12} & A_{22} & 0 & B_{12} & B_{22} & 0 \\ 0 & 0 & A_{66} & 0 & 0 & B_{66} \\ B_{11} & B_{12} & 0 & D_{11} & D_{12} & 0 \\ B_{12} & B_{22} & 0 & D_{12} & D_{22} & 0 \\ 0 & 0 & B_{66} & 0 & 0 & D_{66} \end{bmatrix} \tag{17}$$

Here A_{ij}, B_{ij} and D_{ij} (i, j =1, 2 and 6) are extensional, coupling and bending stiffness for isotropic materials, respectively and can be defined in both layers of the cylindrical shells as:

$$\left(A_{ij}, B_{ij}, D_{ij}\right) = \int_{-h/2}^{0} Q_{ij}^{fgm1}\left(1, Z, Z^2\right)dz + \int_{0}^{h/2} Q_{ij}^{fgm2}\left(1, Z, Z^2\right)dz \tag{18}$$

Reduced stiffness matrix Q determines by (19):

$$Q_{11} = Q_{22} = \frac{E}{1-\upsilon^2}$$

$$Q_{12} = \frac{\upsilon E}{1-\upsilon^2} \tag{19}$$

$$Q_{66} = \frac{E}{2(1+\upsilon)}$$

Displacement functions u, v and w considered as follow:

$$u = A_{mn} \cos\left(\lambda x\right)\cos\left(n\theta + \omega t\right)$$

$$v = B_{mn} \sin\left(\lambda x\right)\sin\left(n\theta + \omega t\right) \tag{20}$$

$$w = C_{mn} \sin\left(\lambda x\right)\cos\left(n\theta + \omega t\right)$$

$$\lambda = m\pi / L$$

A_{mn}, B_{mn} and C_{mn} are constant modes of shape coefficient, m is the number of half − wave longitudinal wave and n is the number of half −wave circumferential waves. By substituting equation (18) and (19) into (17), the stiffness matrix of the shell is calculated and by substituting equation (20) in Sanders' strain equations, the strain vector is calculated, and then according to equation (14), the potential energy of the shell can be obtained. The total energy of the system is given as follows:

$$\Pi = T - U_h - U_\varepsilon \tag{21}$$

Using the Ritz minimizing method,

$$\frac{\partial \Pi}{\partial \Delta} = 0 \qquad \Delta = A_{mn}, B_{mn}, C_{mn} \tag{22}$$

The following matrix relation is extracted:

$$\begin{bmatrix} \alpha_{11} & \alpha_{12} & \alpha_{13} \\ \alpha_{21} & \alpha_{22} & \alpha_{23} \\ \alpha_{31} & \alpha_{32} & \alpha_{33} \end{bmatrix}\begin{bmatrix} A \\ B \\ C \end{bmatrix} = \begin{bmatrix} 0 \\ 0 \\ 0 \end{bmatrix} \tag{23}$$

That α_{ij} are the constants. For obtaining a non-trivial answer of the aforementioned equations, the determinant matrix must be zero. After expanding determinant, the characteristic equations of membrane frequencies can be obtained as follows:

$$\beta_1 \omega_{mn}^6 + \beta_3 \omega_{mn}^4 + \beta_4 \omega_{mn}^3 + \beta_5 \omega_{mn}^2 + \beta_6 \omega_{mn} + \beta_1 = 0 \tag{24}$$

After solving equation (24), the natural frequencies of shell is extracted.

4. Results and discussion

4.1. *Materials*

Material properties listed in this study is expressed in table 1.

Table 1: Material properties of FGM [24]

Material	Coefficients	P_0	P_{-1}	P_1	P_2	P_3	P
Stainless steel (SS)	$E(N\ m^{-2})$	201.04×10^9	0	3.079×10^{-4}	-6.534×10^{-7}	0	2.07788×10^{11}
	ν	0.3262	0	-2.002×10^{-4}	3.797×10^{-7}	0	0.317756
	$\rho(kg\ m^{-3})$	8166	0	0	0	0	8166
Nickel (Ni)	$E(N\ m^{-2})$	223.95×10^9	0	-2.794×10^{-4}	-3.998×10^{-9}	0	2.05098×10^{11}
	ν	0.3100	0	0	0	0	0.3100
	$\rho(kg\ m^{-3})$	8900	0	0	0	0	8900
Zirconia (Zr)	$E(N\ m^{-2})$	244.27×10^9	0	-1.371×10^{-3}	1.214×10^{-6}	-3.681×10^{-10}	1.6806296×10^{11}
	ν	0.288	0	1.133×10^{-4}	0	0	0.297996
	$\rho(kg\ m^{-3})$	5700	0	0	0	0	5700
Alumina (Al_2O_3)	$E(N\ m^{-2})$	349.55×10^9	0	-3.853×10^{-4}	-4.027×10^{-7}	-1.673×10^{-10}	3.8×10^{11}
	ν	0.30	0	0	0	0	0.30
	$\rho(kg\ m^{-3})$	3800	0	0	0	0	3800

4.2. *Validation*

The accuracy and precision of the results in this study are evident when compared with results of previous studies. Table 2 shows the natural frequencies of five types of FGM bi-layered shells with non-dimensional geometric parameters L/R = 20, h/R = 0.002, longitudinal wave number (m) = 1, circumferential wave number (n) = 1,2,3,4,5 and power law index (N) = 5 as compared with the results of Arshad et al. [11].

Table 2: Comparison of natural frequencies (Hz) with circumferential wave number n for power law exponent N =5 with geometrical parameters*(m=1,h/R=0.002,L/R=20)* for simply supported Bi-layer FGM cylindrical

Material	Ni-Zr-SS		Ni-SS-Zr		SS-Ni-Zr		SS-Zr-Ni		Zr-Ni-SS	
n	Ref.[11]	Present	Ref.[11]	Present	Ref.[11]	Present	Ref.[11]	Present	Ref.[11]	Present
1	13.645	13.645	13.322	13.321	13.266	13.265	13.915	13.914	13.512	13.512
2	4.6257	4.6222	4.5108	4.5110	4.4853	4.4852	4.7113	4.7070	4.5808	4.5827
3	4.3313	4.3185	4.1502	4.1509	4.1284	4.1281	4.4087	4.3923	4.2154	4.2234
4	7.3665	7.3509	7.0123	7.0130	6.9889	6.9886	7.5069	7.4870	7.1114	7.1213
5	11.775	11.758	11.198	11.198	11.168	11.167	12.005	11.983	11.35	11.36
Average error = 0.09 %										

Table 3 shows the natural frequencies of a single-layered FGM cylindrical shell at different rotation speeds (0 to 200 rev/s) [18]. The frequencies were extracted for a shell composed of Al-Al_2O_3 for m = n = 1 modes.

Table 3: Comparison of natural frequency for a rotating single layer FGM cylinder
(h/R=0.01,L/R=3,N=1,n=m=1, AL-Alumina)

F_f (Hz)		F_b (Hz)		Ω(rad/s)
Ref [18]	Present	Ref [18]	Present	
518	516.97	518	516.97	0
493.8	492.82	542.13	541.11	25
469.56	468.66	566.2	565.23	50
420.91	420.29	614.16	613.43	100
372.07	371.87	661.85	661.56	150
323.04	323.39	709.22	709.63	200
Average error = 0.14 %				

Table 3 shows two columns for each rotating speed that reflects forward and backward frequencies. Indeed, rotation in the positive direction presents a decreasing behavior in the natural frequencies and rotation in the negative direction presents an increasing behavior in the natural frequencies. Hence, the natural frequencies of

rotating cylinder versus rotational speed bifurcate into two branches as the forward and backward whirl, respectively. The average values of the errors in Tables 2 and 3 are confirmation of the results of the present study when compared with results of previous studies.

4.3. *Effect of increase in the number of layers on critical speed*

In the related figures to the critical speed, the lower branch corresponds to the forward whirl and the upper branch corresponds to the backward whirl. The critical speed of the rotating shell corresponds to the rotational speed of the shell at the point where the forward mode intersects the abscissa. At this intersection, unstable phenomena may exist as the forward mode ceases for the travelling θ coordinate in preparation to switch to backward mode. At this critical speed, any residual unbalance will synchronize with the rotation and magnify the whirling amplitude. The results of the present study and other studies on critical speed confirm that this phenomenon only occurs at n = 1[14]. The results of the present study for critical speed in this mode were extracted and the effects of the different parameters on them was analyzed.

Figure 3 shows the forward and backward natural frequencies for a single-layered shell (Ni-SS) and bi-layered shell (Ni-alumina-SS) for rotation speeds of 0 to 2000 (rad/s) at n = m = 1 with non-dimensional geometric parameters L/R = 6 and h/R = 0.002 and power law index N = 1.
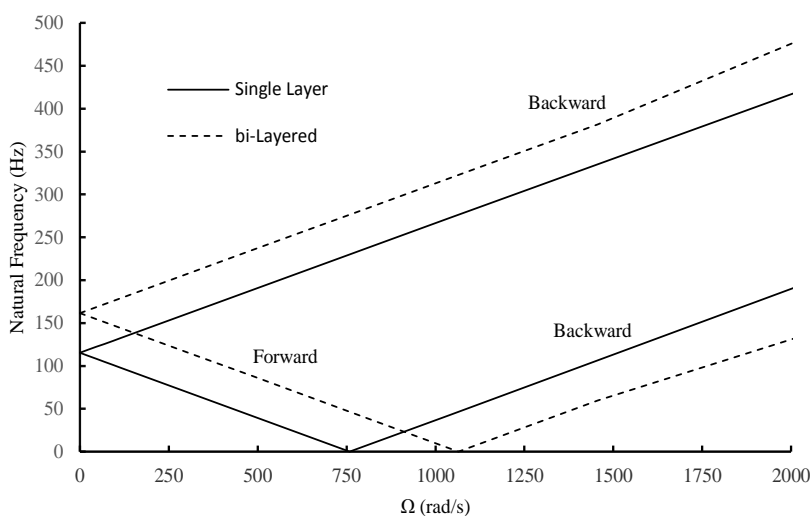
Figure 3: Variation of natural frequencies of a single layer (Ni -SS) and bi-layered (Ni-Alumina-SS) FGM Cylindrical shell versus Ω (L/R=6, h/R=0.002, n=m=1, N=1)

As shown, at different rotation speeds, the natural frequencies of the bi-layered FGM shell are higher than those of the single-layered FGM shells. This is a major finding of the present study. Increasing one alumina layer without changing the total thickness of the shell increased the critical speed about 40% and its vibrational characteristics were substantially improved.

4.4. *Effect of mode on critical speed*

Figures 4 and 5 show the bifurcations of the natural frequencies for the transverse modes of (m,n) = (1,1), (1,2), (1,3) and (m,n) = (2,1), (2,2), (2,3) for bi-layered FGM shells of Ni-alumina-SS material and non-dimensional geometric parameters L/R = 6 and h/R = 0.002, respectively. Critical speed only occurred at n = 1; at higher circumferential modes, there was no critical speed. Increasing the rotation speed increased the distance between the forward and backward modes. When Ω = 0, increasing n decreased the natural frequencies, but increasing the rotation speed reversed these results; for example, at a rotation speed greater than 485 (rad/s) the backward frequency at n = 3 is higher than at n = 1 and n = 2. Comparison of Figures 4 and 5 reveals that the effect of rotation speed in higher longitudinal wave numbers is greater on critical speed and natural frequencies.

Figure 6 shows the natural frequencies and critical speed based on the number of longitudinal waves m = 1, 2, 3, 4, 5 at n = 1 for a bi-layered FGM shell made of Ni-alumina-SS and non-dimensional geometric parameters L/R = 6 and h/R = 0.002. As seen, an increase in the number of longitudinal waves from 1 to 5 increased the critical speed of the shell and the increase was larger at lower longitudinal wave numbers. Figure 6 also shows that the backward frequencies at the top of the chart at high rotation speeds and the number of high longitudinal waves approach each other.
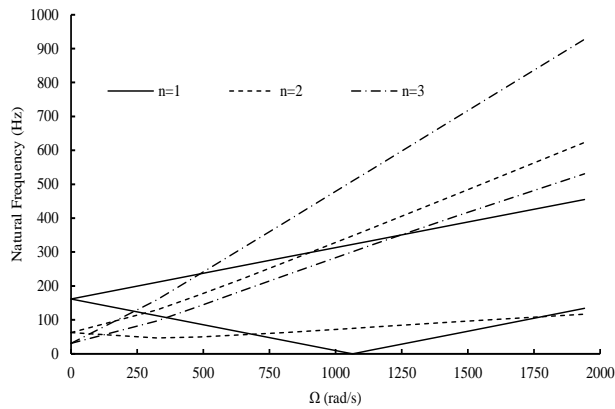
Figure 4: Variation of natural frequencies of a bi-layered (Ni-Alumina-SS) FGM Cylindrical shell versus Ω (L/R=6,h/R=0.002, m=1, N=1)
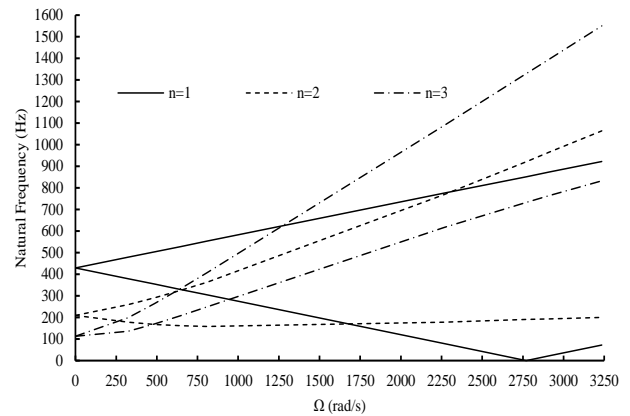
Figure 5: Variation of natural frequencies of a bi-layered (Ni-Alumina-SS) FGM Cylindrical shell versus Ω (L/R=6,h/R=0.002, m=2, N=1)
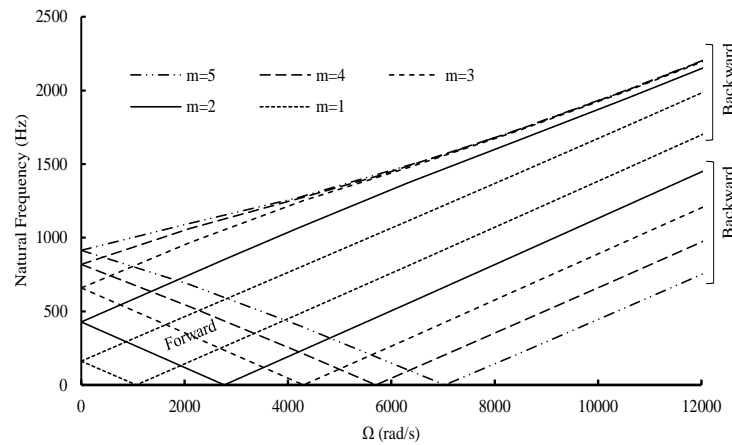
Figure 6: Variation of natural frequencies of a bi-layered (Ni-Alumina-SS) FGM Cylindrical shell versus Ω (L/R=6, h/R=0.002, n=2, N=1)

4.5. *Effect of power of law index on critical speed*

The power law index (N) effects the vibration and critical speed of a cylindrical shell made of functionally graded materials. Table 4 shows that an increase in N for both single layered and bi-layered shells decreased the critical speed. For each value of N, the addition of one alumina layer significantly increased the critical speed for different numbers of longitudinal wave numbers. For example at N = 0.01 and m = 1, the conversion of a shell from single-layered to bi-layered (without changing the total thickness) increased the critical speed about 39%.

Table 4: Critical speed of a rotating bi-layered (Ni-Alumina-SS) and single layer (Ni-SS) FGM cylinder (h/R=0.002, L/R=6, n=1)

m=2		m=1		N
Ni-Alumina-SS	Ni-SS	Ni-Alumina-SS	Ni-SS	
2814.528571	2022.138	1081.494216	777.4847	0.01
2811.006315	2018.296	1080.148616	775.998	0.05
2806.994846	2013.909	1078.613968	774.3005	0.1
2785.06388	1989.784	1070.191907	764.9649	0.5
2770.429967	1973.617	1064.549891	758.7084	1
2749.038278	1949.972	1056.281036	749.5582	3
2744.832396	1945.327	1054.65301	747.7608	4
2742.041023	1942.246	1053.572114	746.5684	5
2738.565668	1938.411	1052.226024	745.0845	7
2737.410584	1937.137	1051.778544	744.5915	8
2735.733434	1935.287	1051.128743	743.8757	10
2733.380834	1932.694	1050.217099	742.8721	15

4.6. *Effect of geometric parameters on critical speed*

Figure 7 shows the critical speed of the Ni-SS circular single-layered FGM shell and bi-layered Ni-alumina-SS versus non-dimensional ratio L/R. The critical speed of the shell rapidly decreased as the L/R ratio increased and at higher L/R ratios the values became nearly constant. Adding an alumina layer and converting the shell from single-layered to bi-layered in longitudinal modes 1 and 2 increased the critical speed. This increase was significant at low L/R values and was less at high L/R values. The effect of increasing the number of layers on critical speed at higher m values was larger.
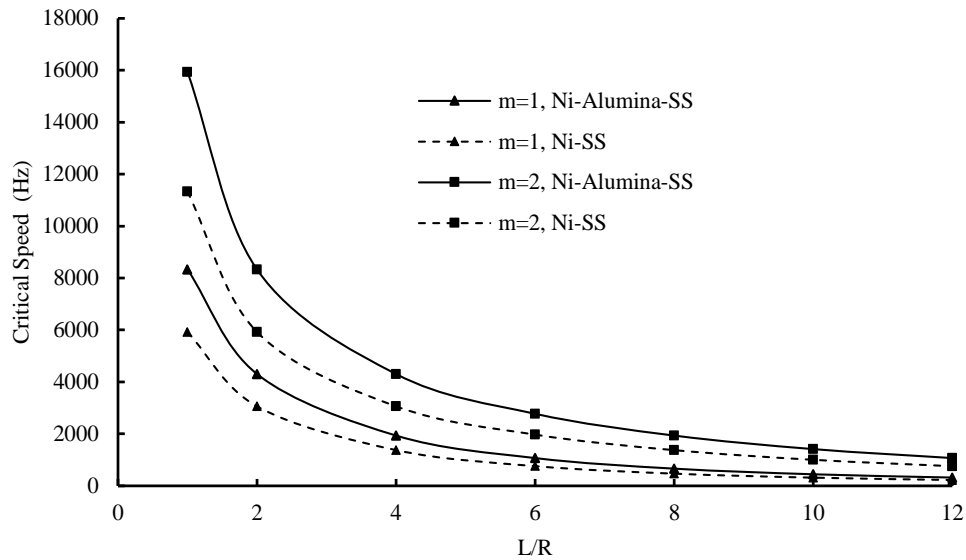
Figure 7: Variation of critical speed of a single-layer and bi-layered FGM Cylindrical shell versus L/R ratio
(h/R=0.002, N=1, n=1)

4.7. *Effect of combined materials in layers on critical speed*

Figure 8 shows the effect of different combinations of layer materials on the critical speed of a circular FGM shell. For each arrangement, the critical speed point changes, which shows the strong effect of combined materials on the critical speed of the shells. The high modulus of elasticity and low density of the ingredients had a significant effect on critical speed. The combinations in Figure 8 showed the highest critical speed was recorded for the Al-alumina-Zr bi-layered shell and the lowest critical speed for the Ni-Zr-alumina shell.
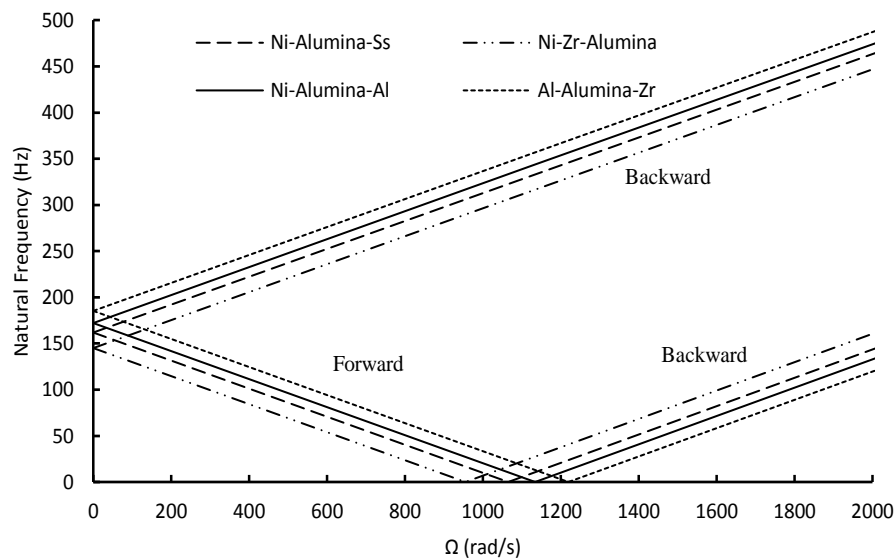
Figure 8: Variation of natural frequencies of a bi-layered FGM Cylindrical shell versus Ω
(L/R=6, h/R=0.002, m=n=1, N=1)

Conclusions

This study analyzed the critical speed of rotating bi-layered circular cylindrical shells made of functionally graded materials. To extract the movement equations, the Sanders' thin shells theory was used while considering the Coriolis effects, centrifugal force and initial hoop tension. The effect of different parameters on the critical speed was studied and the results extracted. It can be seen that, at different rotating speeds, the natural frequencies of the bi-layered FGM shells were higher than for those of the single-layered FGM shells and their vibrational characteristics improved remarkably. The longitudinal wave number had a great effect on critical speed. It was observed that the critical speed of the shell increased as m increased and that the amount of increase was greater for lower longitudinal wave numbers. An increase in N in single- or double-layered shells decreased the critical speed. The critical speed of the shell rapidly decreased as the L/R ratios increased; at higher L/R ratios, the values were nearly constant. The mechanical properties of the layer materials had a strong effect on the point of critical speed of the shell.

References

1. Loy C. T., Lam K. Y., Reddy J. N., *Int. J. Mech. Sci.,* 41 (1999) 309.
2. Pradhan S. C., Loy C. T., Lam K. Y., Reddy, J. N., *App. Acoust.,* 61 (2000) 111.
3. Santos H., Soares C. M. M., Mota Soares C. A., Reddy J. N., *Compos. Structut.,* 86 (2008) 10.
4. Iqbal Z., Naeem M. N., Sultana N., *Acta Mech.,* 48 (2009) 208.
5. Arjangpay A., R. Ansari darvizeh M., *Modares Mech. Eng.,* 12 (2013) 80.
6. Golpayegani I. F., Gorbani E., *JMES.,* 7 (2016) 981.
7. Li S. R., Fu X. H., Batra R. C., *Mech. Res. Commun.,* 37 (2010) 577.
8. Sofiyev A. H., Deniz A., Akeay I. H., Yusufoglu E., *Acta Mech.,* 183 (2006) 129.
9. Arshad S. H., Naeem M. N., Sultana N., Iqbal Z., Shah A. G., *J. Mech. Sci. Technol.,* 24 (2010) 805.
10. Sepiani H. A., Rastgoo A., Ebrahimia F., Arani A. G., *Mater. Design,* 31 (2010) 1063.
11. Arshad S. H., Naeam N. M., Sultana N., Shah A. G., Iqbal Z., *Arch. Appl. Mech.,* 81 (2011) 319.
12. Shah A. G., Naeem M. N., Ali A., Mahmood T., Arshad S. H., *Pakistan J. Sci.,* 65 (2013) 256.
13. Kim C. D., Bert C. W., *Compos. Eng.,* 3 (1993) 633.
14. Ng T. Y., Lam K. Y., *App. Acoust.,* 56 (1999) 273.
15. Ahmad M., Naeem M. N., *Eur. J. Sci. Res.,* 36 (2009) 184.
16. Hosseini-Hashemi S., Khorami K., *Modares Mech. Eng.,* 11 (2011) 93.
17. Daneshjou K., Madoliat R., TalebiTooti M., *Modares Mech. Eng.,* 12 (2013) 80.
18. Hosseini-Hashemi S., Ilkhan M. R., Fadaee M., *Int. J. of Mech. Sci.,* 76 (2013) 9.
19. Talebitooti M., Daneshjou K., Talebitooti R., *J. Therm. Stress,* 36 (2013) 160.
20. Civalek O., *Compos. Struct.,* 160 (2017) 267.
21. Mehrparvar M.., *J. Solid Mech.,* 1 (2009) 159.
22. Zhao X., Liew K. M., Ng T. Y., *Int. J. Solids Struct.,* 39 (2002) 529.
23. Sanders J. L., *An improved first-approximation theory for thin shells*: NASA TR R-24, 1959.
24. Hui-Shen S., *Functionally Graded Materials: Nonlinear Analysis of Plates and Shells:* CRC Press, 2011.

(2017) ; http://www.jmaterenvironsci.com